Journal of Solid State Chemistry **144,** 255–262 (1999)
Article ID jssc.1999.8211, available online at http://www.idealibrary.com on IDEAL®

Structural Properties and Thermal Stability of $Bi_8Pb_5O_{17}$ Fast Ion Conducting Phases

Monica Santarosa,* Lara Righi,† Mauro Gemmi,‡,§ Adolfo Speghini,* Andrea Migliori,‡
Gianluca Calestani,† and Marco Bettinelli*,[1]

**Dipartimento Scientifico e Tecnologico, Università di Verona, Ca' Vignal, Strada Le Grazie, 37134 Verona, Italy;*
†Dipartimento di Chimica Generale ed Inorganica, Chimica Analitica e Chimica Fisica and CNR-CSSD, Università di Parma, Viale delle Scienze, 43100 Parma, Italy; ‡CNR-LAMEL, Area della Ricerca di Bologna, Via Gobetti 101, 40129 Bologna, Italy; and
§Dipartimento di Fisica and Instituto Nazionale per la Fisica della Materia, Università di Bologna, Viale Berti Pichat 6, 40127 Bologna, Italy

Received November 17, 1998; in revised form February 3, 1999; accepted February 4, 1999

Samples with $Bi_8Pb_5O_{17}$ stoichiometry were synthesized by ceramic techniques at temperatures ranging from 200 to 640°C. Their structural properties and relative stabilities were investigated using X-ray and electron diffraction, differential scanning calorimetry, and Raman spectroscopy. The tetragonal β_2 phase is described by an incommensurately modulated structure, whose modulation depends on the firing temperature. Heat treatments in the 200–300°C range lead to the formation of a new tetragonal phase, χ, which is converted back to β_2 above 300°C. The intermediate ϕ phase can be obtained without the previous formation of β_2, and its X-ray powder diffraction pattern is indexed using a triclinic cell. The present data suggest that the β_2 phase is the low-temperature polymorph of this composition. © 1999 Academic Press

1. INTRODUCTION

Mixed oxides characterized by relatively high ionic conductivity are promising candidates as electrodes in fuel cells or as membranes which can separate oxygen from air or other gases (1). These membranes are required to be semipermeable to oxygen at high temperature, but not permeable to other gaseous substances. The oxygen migration, due to thermal dissociation of molecules chemisorbed on the oxide surface, is made possible by the joint diffusion of O^{2-} ions, or under the driving force of an oxygen chemical potential gradient (1).

Phases belonging to the Bi_2O_3–PbO binary system have attracted in recent years considerable interest due to their high ionic conductivity (2, 3). Although they are an unlikely candidate for use in fuel cells they may be suitable as oxygen selective membranes (4). This has spurred the investigation of their synthesis and their structural characterization.

An important effort has concentrated on the stoichiometric compound of composition $4Bi_2O_3 \cdot 5PbO$ (2, 5, 6). This composition was found to form several different phases depending on the thermal history of the material.

It was found that above 590°C a disordered cubic phase, labeled as β, is stable (6, 7). The formation of a tetragonal phase, labeled β_2, by cooling β at room temperature, was reported (5–8). This β_2 phase was described in 1939 by Sillen and Aurivillius (9) as a disordered structure with Bi and Pb randomly occupying the same site in an oxygen-deficient lattice. Different possibilities of ordering in the β_2 structure were suggested by different authors (7, 8) and the possible coexistence of disordered β_2 and an ordered (β_3) phase at room temperature was discussed (8). The $\beta_2 \rightarrow \beta$ transition was reported to occur via an intermediate material (ϕ), whose crystal structure was not solved. It was suggested that this material consists of up to three distinct phases (6).

The ionic conductivity of the β phase was found to be very high (> 1 S/cm), whereas the β_2 and ϕ materials show lower conductivity (1, 6). However, the intermediate ϕ appears to be interesting in high-temperature applications requiring supported membranes, due to its favorable thermal expansion coefficient (6).

In this paper we present a comprehensive investigation of the relative stabilities and of the structural properties of these various phases. In particular, we show that the β_2 material has an incommensurately modulated structure, which depends on the temperature, that a new phase (χ) is formed when the β_2 phase is heated at about 200°C and that the ϕ material is a single phase which can be directly obtained by reacting the starting oxides in an appropriate temperature range without the previous formation of the β_2 phase.

---

[1] To whom all correspondence should be addressed. E-mail: bettinel@sci.univr.it.

0022-4596/99 $30.00

2. EXPERIMENTAL

Samples with composition $4Bi_2O_3 \cdot 5PbO$ were synthesized via ceramic techniques using the oxides PbO (Aldrich 99.9 + %) and Bi_2O_3 (Aldrich 99.9%) as reagents. The starting materials were mixed by a dry homogenization technique and then pellets (10 mm diameter and 5 mm thickness) were prepared using a die press. The pellets were then sintered in open alumina crucibles at characteristic temperatures in order to obtain different products.

X-ray powder diffraction (XRPD) was performed on a Philips Xpert system using Ni-filtered Cu$K\alpha$ radiation. The digitized data were collected in the 5–100° range of 2θ with step 0.02–0.05° by applying a counting time of 2–10 s per step.

Selected-area electron diffraction (SAED) and high-resolution electron microscopy (HREM) experiments were performed using a Philips CM 30 transmission electron microscope operating at 300 kV, equipped with a Gatan slow-scan CCD camera. The probes were prepared by mild grinding of the powdered samples and depositing of fine particle suspended in isopropanol on a holey carbon film.

The 488.0-nm line of a Spectra-Physics Stabilite 2017 Argon laser was used to measure room-temperature Raman spectra. A fiber optic probe coupled to a Dilor Superhead, equipped with a suitable notch filter, was employed. The scattered signal was analyzed by a Jobin–Yvon HR460 monochromator and a CCD detector.

Differential scanning calorimetry (DSC) measurements were performed in the temperature range of 20–590°C at different rates ranging from 10 to 40°C $\min^{-1}$ using a Perkin–Elmer DSC 7 equipment.

3. RESULTS AND DISCUSSION

The β_2 phase was obtained following the procedure previously described (6); the sample was sintered for 70 h at 620°C and cooled by air quenching, although other cooling regimes were also examined. Raman spectra measured on the obtained materials were found to be identical to those reported in literature (5, 6, 8, 10). The nature of the crystalline phase was identified from XRPD data (Fig. 1) according to the literature (5, 6, 8, 10). However, some weak peaks (indicated by arrows in Fig. 1), which cannot be indexed on the basis of the tetragonal β_2 unit cell ($a_T = b_T = 4.0417(8)$, $c_T = 5.0146(9)$ Å), were systematically observed in the XRPD pattern of the β_2 phase. The presence of similar peaks previously induced some authors to suggest the existence of structural order in the solid solution. Vikhreva *et al.* (7) interpreted the peaks on the basis of an orthorhombic superstructure having $a = 2a_T\sqrt{2}$, $b = a\sqrt{3}$ and $c = 3c_T$. A tetragonal structure with $a = 6a^T$ and $c = c_T$ is reported in the JCPDS 45-0291 and 46-0002 cards (11, 12) for two almost identical composition $Bi_8Pb_5O_{17}$ and $Bi_{1.23}Pb_{0.77}O_{2.62}$. The coexistence of this superstructure, labeled as β_3, with disordered β_2, was recently suggested (8) in order to explain the presence of the weak unindexed peaks in he XRPD data.

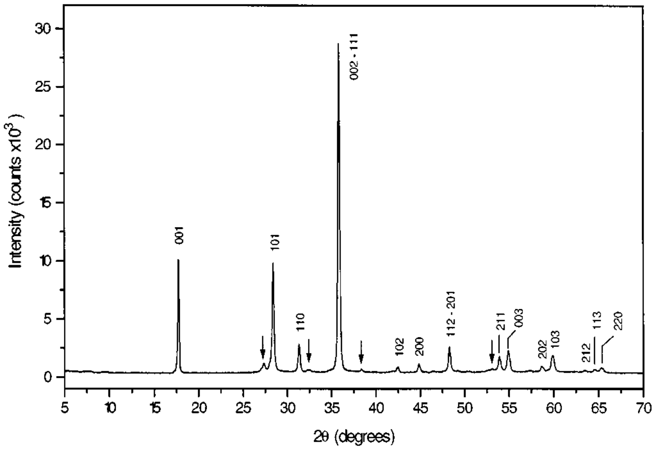

FIG. 1. Powder X-ray diffraction pattern for the β_2 phase indexed on the basis of the fundamental tetragonal cell. Unidexed peaks are indicated by arrows.

We decided to investigate the problem using SAED, that represents the most powerful technique to approach this type of phenomena. On the basis of the SAED study the β_2 phase, obtained by cooling the β phase to room temperature with a 20°C/min rate, was found to be homogeneous and was characterized by an incommensurate tridimensional structural modulation. Figure 2A shows a typical SAED pattern taken in the [001] projection. The fundamental reflections, appearing as the most intense spots in the diffraction pattern, are indexed on the basis of the tetragonal β_2 unit cell. Several satellites, described by the modulation vectors $\mathbf{q}_1 = 0.18\, \boldsymbol{a}_T^*$ and $\mathbf{q}_2 = 0.18\, \boldsymbol{b}_T^*$, are clearly visible in the pattern. The tridimensional character of the structural modulation is clearly evidenced in Fig. 2B, where a [−112] SAED pattern is shown: the indexing of the satellite reflections requires a further modulation vector $\mathbf{q}_3 = 0.5\boldsymbol{c}_T^*$ so that the complete indexing of the diffraction pattern requires a six indexes scheme ($\mathbf{R} = h\boldsymbol{a}_T^* + k\boldsymbol{b}_T^* + l\boldsymbol{c}_T^* + m\mathbf{q}_1 + n\mathbf{q}_2 + p\mathbf{q}_3$, where $\mathbf{R}$ is a general reflection and h k, l, m, n, and p are integer numbers). By taking into account that $\mathbf{q}_1 = \mathbf{q}_2 \approx 1/5\, \boldsymbol{a}_T^*$ and $\mathbf{q}_3 = 1/2\, \boldsymbol{c}_T^*$ the real structure of the β_2 phase could be thought as described by an almost commensurate tetragonal superstructure with $a = 5\, a_T$ and $c = 2\, c_T$. Figure 3 shows a HREM image taken along [001]. The existence of the structural modulation in the *ab* plane leading to the formation of the almost commensurate 5×5 superstructure is clearly visible in the image, whereas the Fourier transform in the inset is perfectly compatible with the diffraction pattern in Fig. 2A. Because the scattering amplitude of bismuth and lead are almost equivalent for

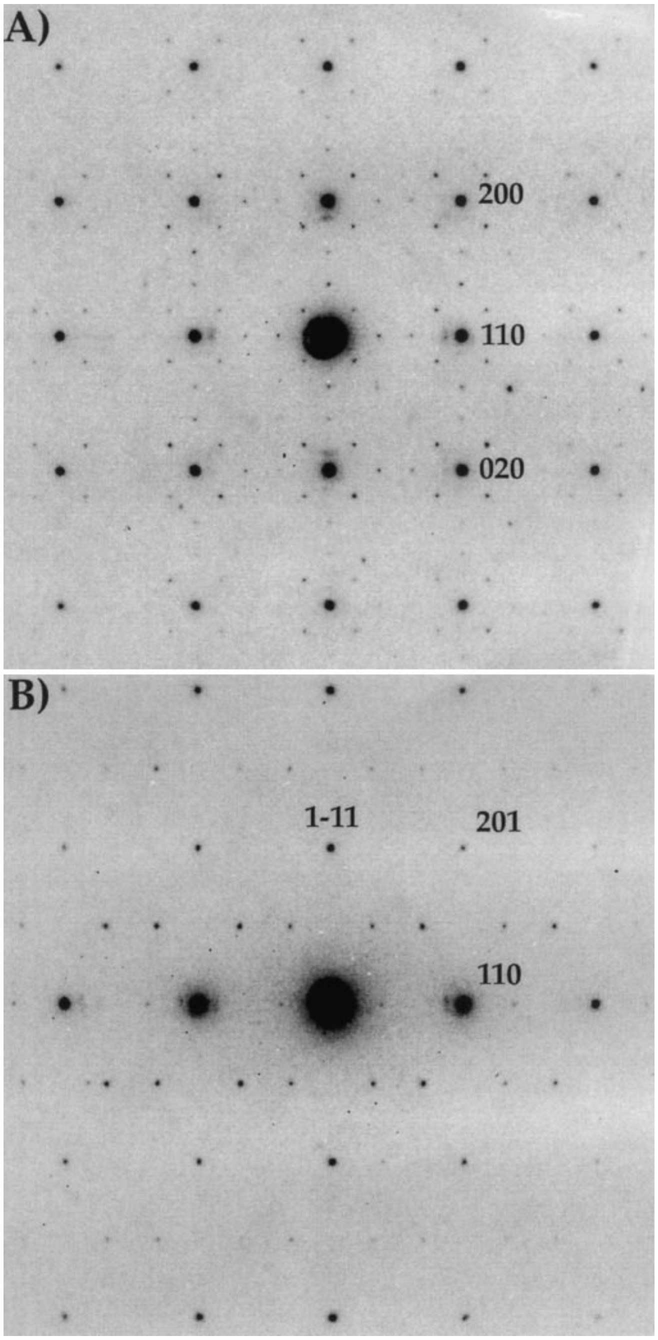

FIG. 2. (A) [001] and (B) [−112] SAED pattern for the β_2 phase indexed on the basis of the fundamental tetragonal cell. Satellite reflections produced by the incommensurate modulation are clearly visible.

both X-ray and electrons, a simple ordering of Bi and Pb atoms in the lattice of the real structure is probably insufficient to justify the effects detected in the electron diffraction and HREM experiments. To this purpose, the ordering of oxygen atoms connected with displacement of the heavy atoms from their ideal position in the fundamental β_2 structure should probably be invoked. A detailed investigation of the structural properties of this phase using SAED and single-crystal XRD data is in progress and will be reported elsewhere (13). In any case, the results we obtained point out that the presence of additional peaks in the XRPD pattern of the β_2 phase, which resulted to be an homogeneous material, is accounted for by the modulation of the structure.

The thermal stability and evolution of β_2 were investigated by combining thermal treatments at different temperature and rates, XRPD, SAED, and thermal analysis techniques. DSC analyses of β_2 were performed up to 600°C, in static atmosphere and at various heating rates (Fig. 4). Inspection of Fig. 4 shows that different results were obtained as a function of the heating rate. The DSC analysis carried with a heating rate of 10°C/min shows the presence of a main endothermic effect peaking at 529°C. This temperature is on one hand too high to be attributed to the $\beta_2 \rightarrow \phi$ transition, since we observed that heat treatments carried out on the β_2 phase at 420°C for 1 h already yield the ϕ phase as single product (Fig. 5). On the other hand, it is too low to be attributed to the $\phi \rightarrow \beta$ transition, which has been reported to occur at 590°C (6, 8). The possible nature of this peak will be discussed later. We point out that no exothermic effect at about 480°C is observed in our experiments. Such a peak was detected by Fee *et al.* (6) in the differential thermal analysis of the pure β_2 phase and was attributed to the $\beta_2 \rightarrow \phi$ transition. However, we recorded a very broad endothermic effect just above 400°C, which could be related to this transition. The broadness of the thermal effect is connected to the slow reaction kinetics experimentally observed. The nature (endothermic–exothermic) of the thermal effect related to the $\beta_2 \rightarrow \phi$ transition occurring above 400°C is extremely important, since it is connected with the thermodynamic stability of the phases. It has been stated in the literature that the ϕ phase can only be obtained by annealing of β_2 (6). However, in agreement with the previously reported observations, we point out that the direct reaction of a mixture of the starting oxides of $4Bi_2O_3 \cdot 5PbO$ composition in an appropriate temperature range below the $\phi \rightarrow \beta$ transition temperature, can indeed produce the ϕ phase. Nevertheless, owing to the slow kinetics of the solid-state reaction, that in this thermal range is strongly temperature dependent, the formation of ϕ becomes almost quantitative for a reaction time of 12 h only above 550°C as shown in Fig. 6. Moreover, the heat treatment of a mixture of the starting oxides of $4Bi_2O_3 \cdot 5PbO$ composition for 2 h at 640°C followed by slow cooling to room temperature with a rate of 1°C/min yields in our experiments a material whose XRPD pattern is unmistakably that of ϕ. From all these observations it can be concluded that the ϕ phase is thermodynamically stable at least in the 400–590°C range and that the formation of β_2 by rapid cooling of β is produced by its faster growth kinetics. Two different hypotheses can be suggested for β_2: (a) it is

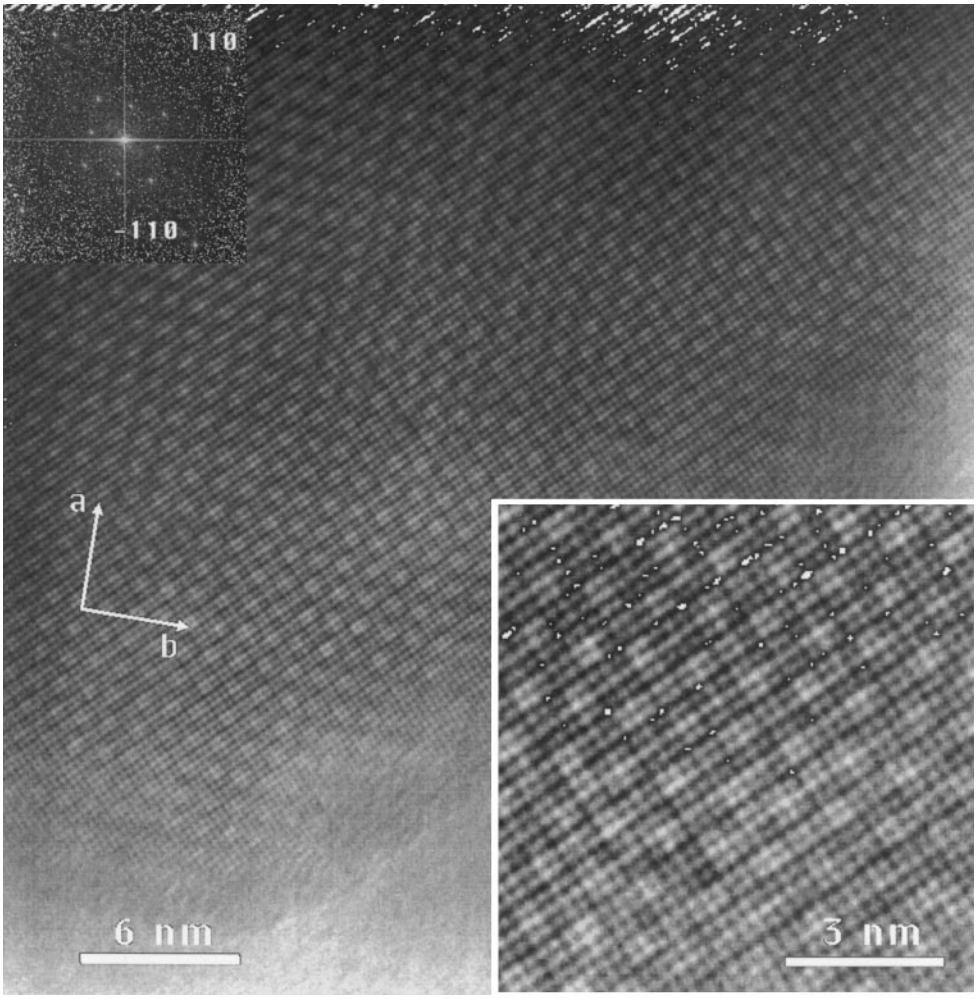

FIG. 3. HREM image of the β_2 phase taken along [001] showing in the real space the existence of a structural modulation. The corresponding calculated Fourier transform, in good agreement with the experimental SAED in Fig. 2A, is shown in the top-left inset. An enlargement of the HREM image is shown in the bottom-right inset.

metastable in the whole temperature range under investigation (ϕ is stable even below 400°C) and (b) is it stable below 400°C and the $\phi \rightarrow \beta_2$ transition is not observed during the slow cooling for kinetic reasons. The presence of the broad endothermic peak in our DSC pattern suggests (b) as the most probable hypothesis. The knowledge of the structure of ϕ could supply further important information.

The nature of the structure of ϕ was extensively investigated using SAED, and more than 30 independent diffraction patterns were taken by using different crystals. All SAED data can unambiguously be indexed (14) by means of a triclinic cell which was refined using the consequently indexed XRPD pattern to $a = 7.458(2)$, $b = 14.190(5)$, $c = 7.215(2)$ Å, $\alpha = 97.19(2)$, $\beta = 118.48(1)$, $\gamma = 80.63(2)°$. The complete structural determination of ϕ is in progress and will be reported elsewhere (13). The observed and calculated reflections for the XRPD pattern are reported in Table 1. By taking into account that the density of ϕ should be comparable with that of β and β_2 it can be concluded that the unit cell of ϕ contains 16 heavy atoms. Since this number is not commensurable to the Bi/Pb ratio in the chemical composition, a peculiar ordering of the oxygen atoms could be involved in the phase formation. The volume per heavy atom is 41.33(2) Å^3, close (but lower) to β (41.39(1) Å^3, JCPDS 45-0295(11)) and significantly larger than that calculated for the fundamental β_2 structure (40.96(1) Å^3). Following the normal trend of the phase transitions, the β_2 phase could be considered the low temperature polymorph, a further support to the previous (b) hypothesis.

Whereas the broad endothermic peak (450–490°C) in the DSC analysis carried out with a heating rate of 10°C/min could be reasonably assigned to the $\beta_2 \rightarrow \phi$ transition, the origin of the further endothermic peak at 529°C, i.e., above the onset of the $\beta_2 \rightarrow \phi$ transition, remains obscure. On the

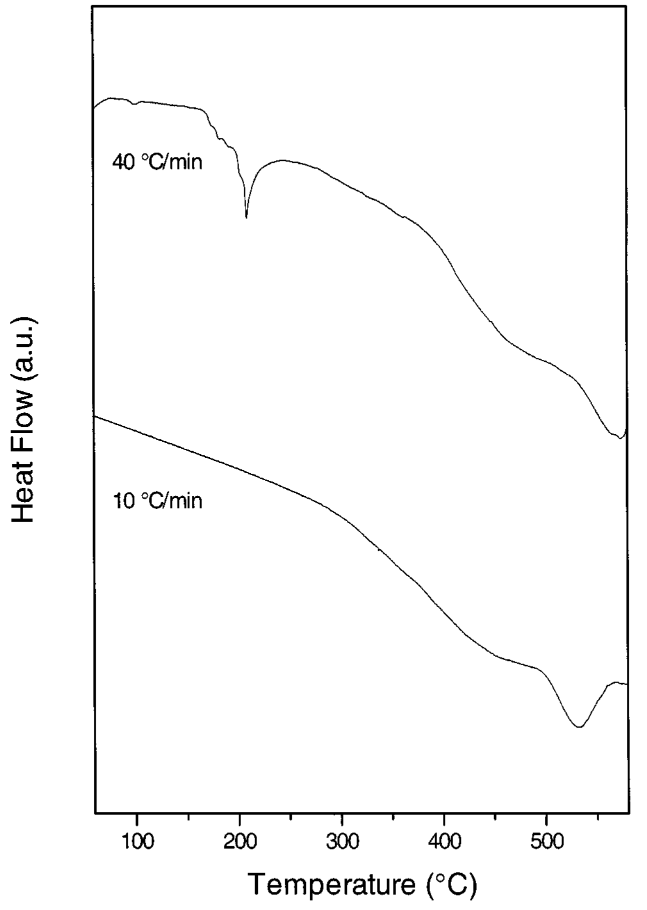

FIG. 4. DSC patterns obtained at different heating rates on β_2 samples.

other hand, DSC analyses carried out on the ϕ phase are not characterized by the presence of this peak. A corresponding peak, accompanied by a weight loss, has been observed by Braileanu *et al.* (10) in the case of the DSC analysis of the starting PbO–Bi_2O_3 mixture of the same composition.

In view of these discrepancies, the temperature range of this thermal effect was investigated in more detail. ϕ samples were treated at different temperatures in the 500–550°C range and XRPD patterns were collected after rapid quenching. No significant variation of the typical ϕ pattern was detected, so that a macroscopic structural rearrangement can be excluded. We could conjecture that the endothermic peak at 529°C is a component of the $\beta_2 \rightarrow \phi$ transition and that it reflects the fact that this transition becomes fast above 500°C. However, it has been shown by Sammes *et al.* that depending on the temperature the system shows a different defective structure (15) and that for several phases belonging to the PbO–Bi_2O_3 system the majority charge carrier is the oxygen ion (16). For this reason, the thermal effect at 529°C could be attributed not to a macroscopic transition, involving a structural rearrangement of the heavy Bi and Pb atoms, but to a local arrangement of the oxygen ions, related to a possible change of the oxygen stoichiometry. This rearrangement of ϕ would occur only

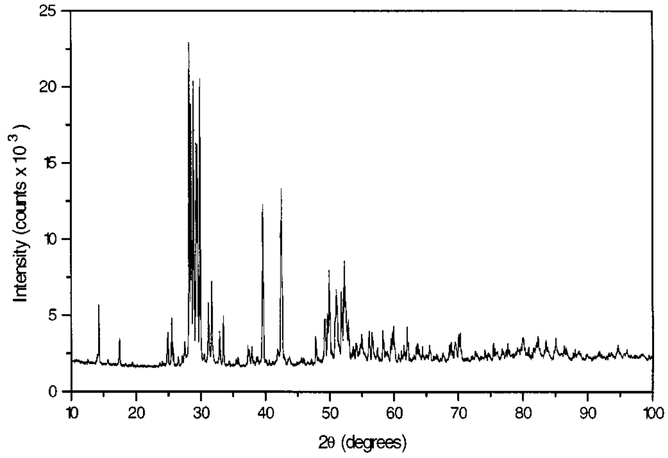

FIG. 5. Powder X-ray diffraction patterns for the ϕ phase.

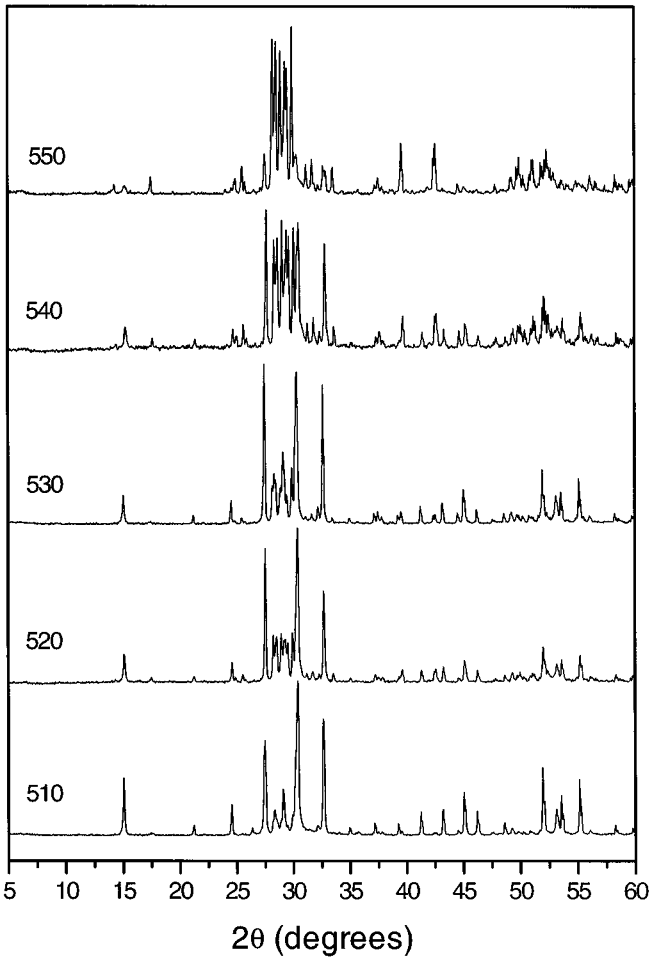

FIG. 6. Powder X-ray diffraction patterns of the reaction product of a mixture of the starting oxides of the $4Bi_2O_3 \cdot 5PbO$ composition treated at different temperatures for 24 h.

TABLE 1

Observed and Calculated d_{hkl} (Å) with Relative Intensities for the XRPD Pattern of the ϕ Phase in the 2θ Range 10–43°

h	k	l	d_{obs}	d_{calc}	I/I_0
0	2	0	7.011	6.990	2
0	0	1	6.332	6.333	4
1	0	−1	6.196	6.212	19
1	1	0		6.188	
1	−1	0	5.646	5.651	3
0	1	1		5.653	
1	2	−1	5.079	5.083	9
1	2	0		5.073	
0	2	−1	4.823	4.826	1
0	2	1	4.573	4.570	2
1	0	1	3.756	3.749	1
2	1	−1	3.704	3.707	1
1	0	−2	3.576	3.578	10
1	1	−2		3.577	
2	2	−1	3.496	3.499	15
0	4	0		3.495	
1	−3	−1	3.460	3.461	5
1	−1	−2	3.365	3.365	3
1	2	−2		3.363	
1	4	−1	3.289	3.289	3
1	4	0	3.242	3.243	7
0	0	2	3.167	3.167	100
2	3	−1		3.149	
2	1	−2		3.145	
0	4	−1	3.133	3.133	80
2	2	0	3.093	3.094	87
2	−1	0		3.090	
2	−2	−1	3.052	3.051	70
0	1	2		3.052	
1	−2	−2	3.031	3.033	60
2	2	−2		3.032	
1	3	−2		3.030	
0	4	1	2.991	2.991	86
2	−1	−2	2.931	2.931	4
1	−3	1	2.872	2.871	20
1	−4	−1		2.850	
2	−2	0	2.826	2.826	26
0	2	2		2.826	
1	5	−1	2.725	2.725	10
1	−3	−2	2.678	2.679	15
2	−3	−1		2.678	
2	−2	−2		2.678	
1	4	−2		2.676	
0	5	−1	2.611	2.611	2
2	4	0	2.531	2.536	2
2	−3	0		2.532	
1	−4	1	2.511	2.511	3
3	2	−1	2.413	2.412	6
0	4	−2		2.413	
1	1	2	2.400	2.400	5
2	−1	1		2.399	
1	−1	2		2.398	
2	2	1	2.376	2.376	6
1	0	−3	2.356	2.356	2
1	−4	−2		2.355	
2	0	−3	2.337	2.337	3
3	−1	−1		2.334	
2	−2	1	2.277	2.276	50
2	5	−2	2.270	2.275	30
2	−1	−3	2.252	2.252	2
2	3	1	2.243	2.243	2
2	3	−3	2.224	2.223	2
1	3	−3	2.197	2.196	1
3	−2	−1		2.193	
1	−3	2	2.155	2.156	5
3	4	−1		2.156	
0	5	−2		2.155	
2	6	−1	2.134	2.134	43
2	−2	−3	2.112	2.121	54

Note. Lattice parameters are $a = 7.458(2)$, $b = 14.190(5)$, $c = 7.215(2)$ Å, $\alpha = 97.19(2)$, $\beta = 118.48(1)$, $\gamma = 80.63(2)°$. The higher 2θ region is not reported due to the severe reflection overlapping.

when this phase is just formed and not when it has aged. Further measurements are being planned to clarify this point.

DSC measurements carried out with a 40°C/min rate shifts the peak previously recorded at 529°C at the limit of the instrumental range of the equipment and makes sharper the broad peak previously attributed to the $\beta_2 \rightarrow \phi$ transition. An additional complex endothermic effect peaking at 208°C was detected and investigated by performing thermal treatments of the β_2 phase at this temperature joined with XRPD analysis. The resulting diffraction pattern is reported in Fig. 7; it shows that in these conditions

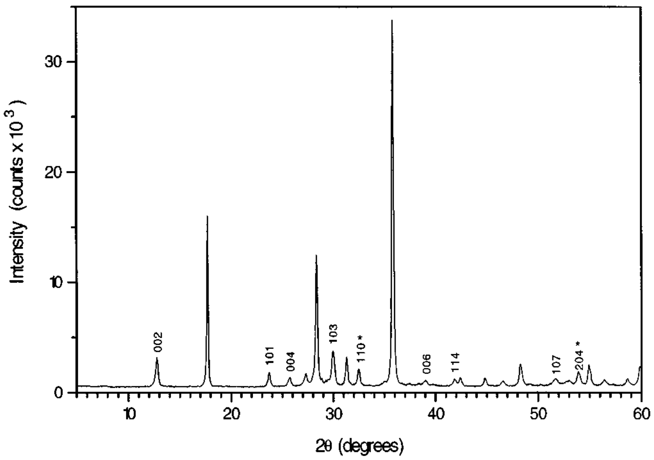

FIG. 7. Powder X-ray diffraction pattern for the mixture χ phase (indexed peaks) and β_2 phase. A star marks the possible overlapping of peaks attributable to both phases.

a mixture of phases seems to be present. The mixture is composed of β_2 and another phase, whose XRPD pattern can be indexed (Table 2) on the basis of an I-centered tetragonal cell with $a = 3.897(1)$ and $c = 13.885(6)$ Å, which is hence lebeled as χ. The detection of the peak at 208°C only in the DSC measurements carried out at a relatively high heating rate (40°C/min) is indicative of a slow process which cannot be evidenced with a slow heating rate, due to its tendency to reach an equilibrium state. Prolonged heat treatments at 208°C do not produce this material as a single phase; on the contrary, an upper limit in the amount of formation of the χ phase seems to be reached. Similar results were obtained by increasing the temperature up to 245°C. By a further increase of the temperature the relative amount of the χ phase starts to decrease and at 300°C the β_2 phase is the unique component on the basis of the XRPD pattern.

No thermal effect, which could be correlated to the reconversion of the β_2 and χ mixture in an apparently pure β_2 phase, was detected in the DSC diagram. It is interesting to note that SAED investigation shows that the β_2 phase obtained in these conditions is still incommensurate, but a decrease of symmetry is observed for the fundamental cell as well as a change in the modulation features. Figure 8 shows a typical SAED pattern taken in the [001] projection of a β_2 sample quenched after a thermal treatment at 300°C. It can be noted that a drastic change in the relative intensity of the 200 and 020 fundamental reflections, which are equivalent in the β_2 cooled down at room temperature, decreases the symmetry of the fundamental pattern from 4*mm* to 2*mm*. A similar effect is detected for the whole diffraction pattern with a dramatic change of the modulation vectors of the satellites surrounding the 020 reflection. The observed dependence of the structural modulation of the β_2 phase on the thermal history suggests a variation of the oxygen content, or at least of the oxygen ordering, with the temperature. This effect should be studied in a detailed way for a better comprehension of the thermal evolution and of the properties of the $4Bi_2O_3 \cdot 5PbO$ system. Unfortunately this requires the knowledge of the real structure of the β_2 phase, whose determination is not simple.

TABLE 2
Observed and Calculated d_{hkl} (Å) with Relative Intensity for the XRPD Pattern of the Tetragonal χ Phase

h	*k*	*l*	$d_{\text{obs.}}$	$d_{\text{cal.}}$	I/I_0
0	0	2	6.935	6.948	50
1	0	1	3.754	3.755	49
0	0	4	3.468	3.468	34
1	0	3	2.984	2.983	100
1	1	0	2.756	2.758	56
0	0	6	2.316	2.316	27
1	1	4	2.161	2.160	35
2	0	0	1.949	1.950	30
1	1	6	1.773	1.773	33
2	0	4	1.701	1.700	51
2	0	6	1.492	1.492	20

Note. The refined lattice parameters are $a = 3.897(1)$ and $c = 13.885(6)$ Å.

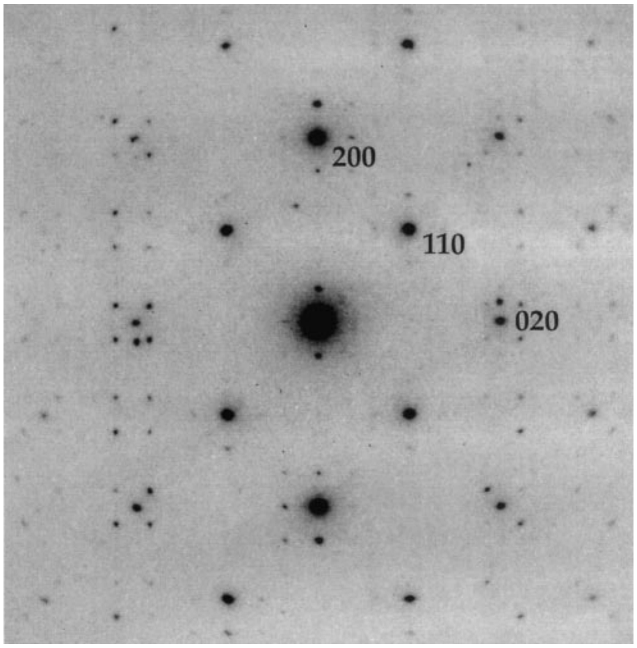

FIG. 8. [001] SAED pattern of the β_2 phase quenched after thermal treatment at 300°C. The pattern is indexed on the basis of the fundamental tetragonal cell. Satellite reflections produced by the incommensurate modulation are clearly visible.

CONCLUSIONS

In this paper we have presented a comprehensive investigation of the crystal structure and of the stability of the fast ion conducting $Bi_8Pb_5O_{17}$ mixed oxide phases. In particular, we have shown that the β_2 phase can be described on the basis of an incommensurately modulated structure and that the modulation changes as a function of the heat treatment temperature. This evidence rules out the existence of an ordered phase, which has been previously labeled as β_3. Thermal treatments around 220°C lead to the formation of an as yet unknown tetragonal phase, which has been labeled χ, and which is converted back to β_2 above 300°C. We report evidence that the ϕ material can be obtained directly and that it is indeed a single phase whose XRPD pattern has been indexed using a triclinic cell. Our results suggest that β_2 can be considered as the low-temperature polymorph of the $Bi_8Pb_5O_{17}$ mixed oxide.

A detailed investigation of the crystal structure of β_2 and ϕ is in progress. These results will allow us to get a deeper insight about the stability of these crystalline phases and the effect of the oxygen stoichiometry and of the structure on their ionic conductivity properties.

ACKNOWLEDGMENTS

The authors gratefully thank Erica Viviani (Università di Verona) and Roberta Magnani (Università di Parma) for expert technical assistance, and Dr. G. Tompsett (The University of Waikato, New Zealand) for communicating the results contained in Ref. (8) prior to publication.

REFERENCES

1. H. J. M. Bouwmeester, H. Kruidhof, A. J. Burggraaf, and P. J. Gellings, *Solid State Ionics* **53–56,** 460 (1992).
2. P. Honnart, J. C. Boivin, D. Thomas, and J. K. De Vries, Solid State Ionics **9–10,** 921 (1983).
3. J. C. Boivin and G. Mairesse, *Chem. Mater.* **10,** 2870 (1998) and references therein.
4. M. G. Fee and N. J. Long, *Solid State Ionics* **86–88,** 733 (1996).
5. N. Sammes, G. Tompsett, and A. M. Cartner, *J. Mater. Sci.* **30,** 4299 (1995).
6. M. G. Fee, N. M. Sammes, G. Tompsett, T. Stoto, and A. M. Cartner, *Solid State Ionics* **95,** 183 (1997).
7. O. A. Vikhreva, I. N. Dubrovina, A. M. Yankin, and V. F. Balakirev, *Russian J. Inorg. Chem.* **38,** 1127 (1993).
8. Y. Du, N. M. Sammes, and G. A. Tompsett, "Proceedings of AUSTCERAM '98, September 28–30, 1998," Monash University, Australia, in press.
9. L. Sillen and B. Aurivillius, *Z. Kristallogr.* **101,** 483 (1939).
10. A. Braileanu, M. Zharescu, D. Crisan, and E. Segal, *J. Therm. Anal.* **49,** 1197 (1997).
11. M. Tromel, K. Grueber, and E. Muench, ICDD Grant-in-Aid, 1991.
12. Grueber, E. Muench, and M. Tromel, ICDD Grant-in-Aid, 1994.
13. G. Calestani *et al.*, unpublished results.
14. D. Belletti, G. Calestani, M. Gemmi, and A. Migliori, "MICRO v 1.0: A program for electron diffraction data treatment," Proc. 28th AIC National Congress, Rimini, Italy, 1998.
15. N. M. Sammes, G. Tompsett, R. Phillips, C. Carson, A. M. Cartner, M. G. Fee, and O. Yamamoto, *Solid State Ionics* **86–88,** 125 (1996).
16. N. M. Sammes, R. J. Phillips, and M. G. Fee, *Solid State Ionics* **69,** 121 (1994).